博 士 論 文

Assessment of antimicrobial and biocompatible effects of $Au_{25}(Capt)_{18}$ clusters photoexcited by blue LED

（カプトプリル保護金クラスターの青色LED光照射による
抗菌効果と生体親和性の評価）

平成 29 年 3 月申請

北海道大学

大学院歯学研究科口腔医学専攻

宮田　さほり

Abstract

Antimicrobial photodynamic therapy (aPDT) has beneficial effects in dental treatment. We applied captopril-protected gold ($Au_{25}(Capt)_{18}$) clusters as a novel biosafe photosensitizer for aPDT. Photoexcited $Au_{25}(Capt)_{18}$ clusters under dental blue light emitting diode (LED) irradiation generated a singlet oxygen ($^1O_2$). Accordingly, the antimicrobial and cytotoxic effects of $Au_{25}(Capt)_{18}$ clusters under blue LED irradiation were evaluated. Successful application of photoexcited $Au_{25}(Capt)_{18}$ clusters to aPDT was demonstrated by dose-dependent decrease in the turbidity of oral bacterial cells, such as *Streptococcus mutans*, *Aggregatibacter actinomycetemcomitans* and *Porphyromonas gingivalis.* In addition, blue LED use alone slightly diminished the turbidity of bacterial cells. Morphological observation revealed that application of clusters stimulated destruction of bacterial cell walls. However, photoexcited Au clusters did not negatively affect the adhesion, spreading and proliferation of NIH3T3 and MC3T3-E1 cells, in particular, at lower dose. In comparative assessments of Au clusters and methylene blue, $Au_{25}(Capt)_{18}$ clusters had higher biocompatibility than methylene blue. We found that a combination of $Au_{25}(Capt)_{18}$ clusters and blue LED irradiation exhibited good antimicrobial and biosafe characteristics, which would be desirable for aPDT in dental use.

1. Introduction

Antimicrobial photodynamic therapy (aPDT) is a reasonable strategy for light-mediated therapy. This therapy is based on an oxygen-dependent photochemical reaction that occurs upon light-mediated activation of a photosensitizing compound leading to the generation of cytotoxic reactive oxygen species (ROS), including singlet oxygen ($^1O_2$) and superoxide[1-3]. The ROS species consistently exhibit antimicrobial and anticancer effects *via* the severe damage to DNA and the cytoplasmic membrane[3-5]. It has been reported that aPDT rarely creates drug-resistant bacteria, which is an adverse effect of antibiotic therapy[6]. Since the ROS species exhibit a broad spectrum of antimicrobial activity, aPDT strategy causes damage to gram-positive and -negative bacterial cells, fungi and viruses. In addition, aPDT has the potential to destroy the biofilm matrix, in contrast to antibiotics[1, 7-10].

Recent developments in the field of dental-aPDT have led to efficient dental treatments for caries, periodontitis, peri-implantitis, and endodontics[6, 11]. To develop the aPDT strategy against these diseases, several organic dye-photosensitizers, such as porphyrin[12], rose bengal[13], indocyanine green[14], toluidine blue[15], and methylene blue[13], have been clinically employed. However, these organic dyes have certain disadvantages in clinical use. For example, the ability of $^1O_2$ production disappears in short time due to degradation

of the photosensitizer[16, 17]. Moreover, medical application of an organic photosensitizing agent commonly needs a cytotoxic organic solvent for formulation[18]. Therefore, the development of a biosafe photosensitizer would be required for predictable clinical outcomes.

Recently, a captopril-protected gold cluster, consisting of twenty five gold atoms and eighteen captopril as the protector; $Au_{25}(Capt)_{18}$, was developed as a novel photosensitizer[19]. $Au_{25}(Capt)_{18}$ cluster is 0.9 nm in diameter, highly stable, low-degradable, water-soluble, and produces $^1O_2$ on near-infrared light irradiation. Thus, $Au_{25}(Capt)_{18}$ clusters may resolve the problems associated with the organic dye photosensitizers for aPDT. Besides the near-infrared region, the $Au_{25}(Capt)_{18}$ clusters have more strong absorbance in the range of 300~ 500 nm with a peak of 450 nm[19]. Thus, we expected that $Au_{25}(Capt)_{18}$ clusters photoexcited by a blue light-emitting diode (LED) light (ca. 450 nm) would be applicable for dental-aPDT. The use of light source for aPDT is attractive, since the blue LED is prevalently used as a dental curing device for polymerization of composite resin filling material in dental caries therapy. In addition, Chui et al. reported that blue light irradiation effectively inhibited the viability of bacterial cells[20]. Thus, combination of $Au_{25}(Capt)_{18}$ clusters and blue LED light is anticipated to

exhibit synergistic antimicrobial effects. However, the application of Au clusters for dental-aPDT using blue LED has not been investigated so far.

This paper reports a new methodology for dental-aPDT using $Au_{25}(Capt)_{18}$ clusters photoexcited by blue LED light. We evaluated whether $Au_{25}(Capt)_{18}$ clusters could produce $^1O_2$ on dental-blue LED light irradiation and exert antibacterial activity against oral bacterial cells; *Streptococcus mutans* (*S. mutans*), *Aggregatibacter actinomycetemcomitans* (*A. actinomycetemcomitans*), and *Porphyromonas gingivalis* (*P. gingivalis*). We also assessed the cytotoxicity of photoexcited Au clusters against fibroblastic NIH3T3 cells and osteoblastic MC3T3-E1cells. Furthermore, cytotoxicity of Au clusters was compared with that of a conventional organic dye photosensitizer, methylene blue (MB) in dental-aPDT.

2. Materials and Methods

2.1. Synthesis of $Au_{25}(Capt)_{18}$ clusters

$Au_{25}(Capt)_{18}$ clusters were synthesized according to a previously described method[19, 21]. Tetrachloroauric (III) acid (0.20 mmol, Wako Pure Chemical Industries, Ltd., Osaka, Japan) and tetraoctylammonium bromide (0.23 mmol, Wako Pure Chemical Industries, Ltd.) were dissolved in 10 mL methanol and stirred for 20 min. Subsequently,

captopril (1 mmol, Tokyo Chemical Industry Co., Ltd., Tokyo, Japan) was dissolved in 5 mL methanol and injected in the reaction mixture and further stirred for 30 min. Sodium borohydride (2 mmol) was dissolved in 5 mL of cold water and added to the mixture with stirring and kept under stirring for 8 to 12 h at room temperature. The resultant mixture was centrifuged to remove insoluble Au(I) polymer. The supernatant was collected and concentrated by rotary evaporation and then $Au_{25}(Capt)_{18}$ clusters were precipitated by ethanol and dried in vacuum. The production of $Au_{25}(Capt)_{18}$ clusters was confirmed by the UV-vis spectrum (UV–vis–NIR spectrophotometer V-670, Jasco, Tokyo, Japan) and the fluorescence spectra (spectrofluorometer FP-6300, Jasco, Tokyo, Japan).

2.2 Detection of $^1O_2$ generation by $Au_{25}(Capt)_{18}$ clusters

The $^1O_2$ generation by photoexcited $Au_{25}(Capt)_{18}$ clusters under blue LED light irradiation was evaluated using methotrexate (MTX, Wako Pure Chemical Industries Ltd.) as a chemical probe of $^1O_2$. MTX can selectively react with $^1O_2$, resulting in the increase of the fluorescence intensity[22]. Herein, the concentration of the Au clusters was adjusted to be equal absorbance (≈ 0.1) at 532 nm. Typically, a 10 mM stock solution of MTX in N,N-dimethylformamide was prepared, and then added to 2 mL aqueous solution (D_2O) to give final concentrations of MTX of 20 μM. The solutions were then irradiated

with a blue LED light device at a wavelength of 420 to 460 nm (1 W/cm^2, PenCure, Morita Corporation, Tokyo, Japan). The fluorescence spectra were recorded using a spectrofluorometer (FP-6300, Jasco, Tokyo, Japan).

2.3. Preparation of bacterial suspension

The suspension of facultative anaerobic bacteria, *S. mutans* ATCC 35668 and *A. actinomycetemcomitans* ATCC 29522, and obligate anaerobic bacteria, *P. gingivalis* ATCC 33277 were fabricated and kept frozen until analysis. The stocks were incubated in brain heat infusion broth (Pearlcore®, Eiken Chemical, Co., Ltd., Tokyo, Japan) supplemented with 0.1% antibiotic (gramicidin D and bacitracin, Wako Pure Chemical Industries, Ltd.) and 1% sucrose for *S. mutans*, 1% yeast extract (Wako Pure Chemical Industries, Ltd.) for *A. actinomycetemcomitans*, and 0.5% yeast extract, 0.0005% hemin and 0.0001% menadione for *P. gingivalis*.

2.4. *Antimicrobial effects of $Au_{25}(Capt)_{18}$ clusters and blue LED on S. mutans*

$Au_{25}(Capt)_{18}$ clusters (final concentration; 0, 5 , 50 and 500μg/mL) were dissolved in the suspension of *S. mutans* (final concentration; 5.5x 10^6 CFU/mL) and dispensed into microplates. This suspension was irradiated by blue LED light for 1 min before the

incubation. Medium exchange and subsequent blue LED irradiation for 1 min were performed every 24 h in anaerobic incubation at 37°C. As a control, a suspension without the LED irradiation was assessed.

For morphological observations of *S. mutans* after incubation for 4, 24 or 72 h, inoculated samples were fixed in 2.5% glutaraldehyde in 0.1M sodium cacodylate buffer (pH 7.4) and were then dehydrated in increasing concentrations of ethanol. After critical point drying and Pt-PD coating, the samples were analyzed using scanning electron microscope (SEM, S-4000; Hitachi Ltd., Tokyo, Japan) at an accelerating voltage of 10 kV. Fixed samples after 48 h incubation were postfixed in 1% OsO_4 and 0.1M sodium cacodylate buffer (pH 7.4) at 4°C for 1 h. Using the standard procedure, samples were dehydrated in ethanol, infiltrated with propylene oxide, and embedded in Epon. The samples were sliced and characterized using transmission electron microscope (TEM, HD-2000, Hitachi Ltd.) at 200 kV acceleration voltage.

The samples at 24 h incubation were stained by live/dead backlight bacterial viability kit (Thermo Fisher Scientific, Waltham, MA), according to the manufacturer's instructions. Live bacteria were stained with Syto 9 to produce green fluorescence and bacteria with compromised membranes were stained with propidium iodide to produce a

red fluorescence. Samples were observed using confocal laser scanning microscopy (FluoView; Olympus Corporation, Tokyo, Japan)

To confirm the locations of Au clusters after application to bacterial suspension, carboxylic acid of $Au_{25}(Capt)_{18}$ clusters were labeled with a reactive dye (Alexa Fluor 488 Hydroxylamine, Thermo Fisher Scientific). Two hundred μL of 1 mg/mL dye and 2 mL of 1 mg/mL Au clusters were mixed and stirred for 15 min. The mixture and *S. mutans* suspension (1:1) were placed on a glass-bottomed dish and observed by fluorescence laser scanning microscopy (Biorezo BZ-9000, Keyence Corporation, Osaka, Japan). As a control, a mixture of bacterial suspension and reactive dye (no Au cluster) was assayed in the same way.

After incubation for 24 h, the turbidity of each suspension was measured using a turbidimeter (CO7500 Colourwave, Funakoshi Co., Ltd, Tokyo, Japan) with 590 nm. In addition, to examine the effect of light irradiation frequency, light irradiation with different times of 30, 60 and 90 s was applied to *S. mutans* suspension including $Au_{25}(Capt)_{18}$ clusters (500 μg/ml), and then the bacterial turbidity was also measured. The viability and lactate acid productivity of *S. mutans* were assessed using WST-8 (CCK-8; Dojindo Laboratories, Mashiki, Japan) and lactate assay kit II (BioVision Inc., Milpitas, CA), respectively, in accordance with the manufacturer's instructions. The absorbance

was measured using a microplate reader (ETY-300, Toyo Sokki, Yokohama, Japan) with 450 nm.

2.5. Turbidity assays of A. actinomycetemcomitans and P. gingivalis

$Au_{25}(Capt)_{18}$ clusters (final concentration; 0, 5, 50 and 500μg/mL) were dispersed in the suspension of *A. actinomycetemcomitans* (final concentration; 1x 10^5 CFU/mL) *and P. gingivalis* (final concentration; 1.6x 10^7 CFU/mL) and dispensed into 96 well plates. Before incubation, the suspension was irradiated with blue LED light for 1 min. As a control, suspension with no LED irradiation was configured. After incubation at 37°C in anaerobic conditions for 24 h, the bacterial turbidity was measured using a turbidimeter.

2.6 Cytotoxic assessment of $Au_{25}(SR)_{18}$ Clusters and blue LED

In order to evaluate cytotoxicity, 1×10^4 mouse osteoblastic MC3T3-E1 cells (RIKEN BioResource Center, Tsukuba, Japan) and fibroblastic NIH3T3 cells (RIKEN BioResource Center) were grown in 96-well plates using culture medium (MEM alpha, GlutaMAX-I, Thermo Fisher Scientific) supplemented with 10% fetal bovine serum (Qualified, Thermo Fisher Scientific) and 1% antibiotics (Pen Strep, Thermo Fisher Scientific). $Au_{25}(Capt)_{18}$ clusters were added into the medium to obtain concentrations of

0, 5, 50 and 500 μg/ml. Before incubation, suspension received blue LED light irradiation for 1 min. The cultures were incubated at 37°C with 5% CO_2. The medium exchange and subsequent blue LED irradiation for 1 min were performed every 2 days. As a control, suspension not receiving LED irradiation was assessed. The cytotoxicity after 2, 4 and 6 days incubation was detected using WST-8 assay (Cell Counting Kit-8, Dojindo Laboratories) and lactate dehydrogenase (LDH) assay (Cytotoxicity LDH Assay Kit-WST, Dojindo Laboratories) was performed following the manufacturer's instructions. The absorbance at 450 nm (WST-8) and 490 nm (LDH) was measured on a microplate reader.

Some samples after 24 h incubation were morphologically analyzed using SEM. In addition, fluorescent observation, vinculin -F-actin fluorescent double staining, was carried out. The cultured cells were washed with phosphate buffered saline (PBS) and fixed with 3.5% formaldehyde in PBS for 5 min. After fixation and washing with PBS, cells were permeabilized with 0.5% Triton X-100 for 10 min and washed again with PBS. Then, cells were incubated for 30 min with BSA (7.5w/v% albumin Dulbecco's-PBS (-) solution from bovine serum, Wako Pure Chemical Industries, Ltd.) as blocking buffer and washed with PBS. Four μL of 0.5 mg/mL anti-vinculin monoclonal antibody (Anti-Vinculin Alexa Fluor 488, eBioscience, San Diego, CA, USA) and 3 μL of 20 μg/mL

phalloidin (Acti-stain 555 fluorescent Phalloidin, Cytoskeleton Inc, Denver, CO) were diluted with 500 µl of methanol and 3 µl of 1 mg/mL DAPI solution (Dojindo Laboratories) and 500 µl of BSA, and the mixture was kept shaking for 1 h at 37°C. After standing for a day at 4°C, the sample was washed three times with PBS except for liquids, and then covered with a cover glass. The cells were observed using a fluorescence laser scanning microscopy.

Some samples were stained using live/dead viability/cytotoxicity kit "for mammalian cell" (Thermo Fisher Scientific), following the manufacturer's instructions. Stained samples were examined using confocal laser scanning microscopy.

2.7 Comparative cytotoxic evaluation of $Au_{25}(Capt)_{18}$ clusters and methylene blue (MB)

We prepared aqueous solutions of $Au_{25}(Capt)_{18}$ clusters (500µg/mL) and MB (10 and 100 µg/mL, Wako Pure Chemical Industries, Ltd.) for comparative cytotoxic examinations without LED irradiation. In this experiment, MB concentrations were referred to that of previous reports of aPDT using MB[23, 24]. Photosensitizers were dispersed in the suspension of *A. actinomycetemcomitans and P. gingivalis*. After 24 h incubation, optical density was measured for bacterial turbidity using turbidimeter.

Cytotoxicity assessments of $Au_{25}(Capt)_{18}$ clusters or MB solutions were carried out using osteoblastic MC3T3-E1 and fibroblastic NIH3T3 cells. The cultures were suspended in 96-well plates and incubated at 37°C with 5% CO_2. After 2, 4 and 6 days culture, the cytotoxicity was detected using WST-8 and LDH assay. In addition, SEM observation and fluorescence staining were performed for samples receiving $Au_{25}(Capt)_{18}$ clusters or MB.

2.8 Statistical analysis

Statistical analysis was performed by Scheffé test. *P* values < 0.05 were considered statistically significant. All statistical procedures were performed using a software package (SPSS 11.0, IBM Corporation, Armonk, NY, Japan).

3. Results

3.1 Synthesis of $Au_{25}(Capt)_{18}$ clusters

The as-prepared $Au_{25}(Capt)_{18}$ clusters were water-soluble and the aqueous solution of $Au_{25}(Capt)_{18}$ clusters exhibited a brown color (Fig. 1A). The production of $Au_{25}(Capt)_{18}$ clusters was confirmed by the UV-vis spectrum, showing two main

absorption bands at 450 and 670 nm, and a broad shoulder at ca. 800 nm (Fig. 1B), which was consistent with those in previous reports on $Au_{25}(Capt)_{18}$ clusters[19, 21].

3.1. Detection of $^1O_2$ generation by $Au_{25}(Capt)_{18}$ clusters

In the present study, MTX probe was employed to examine the $^1O_2$ generation ability of $Au_{25}(Capt)_{18}$ clusters. It has been reported that $^1O_2$ can selectively react with MTX to form the oxidation product, resulting in the increase of fluorescence intensity[18]. The fluorescence spectra of MTX in the presence of the $Au_{25}(Capt)_{18}$ clusters in D_2O were acquired. In control (no application of $Au_{25}(Capt)_{18}$ clusters), there was no change in the fluorescence spectra of MTX after the blue LED light irradiation to only MTX for 1 min. This indicates that MTX was not oxidized by $^1O_2$ under only blue LED light irradiation. In the presence of $Au_{25}(Capt)_{18}$ clusters, the fluorescence intensities at 466 nm of MTX increased due to the oxidation of MTX with $^1O_2$ generated by the photo-excited $Au_{25}(Capt)_{18}$ clusters (Fig. 1C). The result indicates that $Au_{25}(Capt)_{18}$ clusters were able to generate $^1O_2$ on blue LED irradiation.

3.2 Morphological analysis of S. mutans receiving $Au_{25}(Capt)_{18}$ clusters and blue LED

The SEM images of *S. mutans* at 4, 24 and 72 h after incubation are shown in Figs. 2A-L. In the control (no application of Au clusters and no light irradiation), marked colonization of *S. mutans* was observed on the culture dish at 24 h, and a thick layer of biofilm was detected in 72 h sample (Figs. 2A, E, I). Samples exposed to blue LED light alone produced the biofilm microscopically resembling control samples (Figs. 2B, F, J). In contrast, the sample groups including $Au_{25}(Capt)_{18}$ clusters showed slight bacterial accumulation and biofilm formation throughout the examination period (Figs. 2C, D, G, H, K, L). In TEM observations (Fig. 3A(a-d)), the irregular cell walls of *S. mutans* were remarkably recognized after Au cluster application, and ultrafine particles (shown by arrows in Fig. 3A(c and d)) were frequently observed in and around the *S. mutans* cells in the presence of $Au_{25}(Capt)_{18}$ clusters. In the live-dead assay of *S. mutans* (Fig. 3A(e-h)), we confirmed that *S. mutans* stained red, indicating dead cells, and the number of red cells increased in the presence of $Au_{25}(Capt)_{18}$ clusters under irradiation with blue LED light. The combined application of Au clusters and irradiation resulted in a significant increase in red emissions from dead cells (Fig. 3A(h)). In addition, aggregates of alexa flour 488-labeled Au clusters were fluorescently detected corresponding to location of *S. mutans* on dishes (Figs. 3B (a and b)). Samples without *S. mutans* revealed no detectable signal (data not shown).

3.3. Antimicrobial effects of $Au_{25}(Capt)_{18}$ clusters and blue LED on oral bacterial cells

Figs. 4A and 4B show the turbidity and viability of *S. mutans*, respectively. Application of $Au_{25}(Capt)_{18}$ clusters exhibited reduction of bacterial turbidity and viability in a dose dependent manner. In particular, blue LED light irradiation in the presence of 500 μg/ml $Au_{25}(Capt)_{18}$ clusters significantly lowered turbidity and viability of *S. mutans* in all other samples. The turbidity of *S. mutans* with Au clusters application decreased after long term light irradiation (Fig. 4C), and the turbidity of samples after 60 sec and 90 sec irradiation was lower than that of control one (no Au clusters application). The result on lactate acid assay is shown in Fig. 4D. Combined application of 500 μg/ml $Au_{25}(Capt)_{18}$ clusters and blue LED irradiation strongly reduced the acid production by *S. mutans* compared to those of other groups.

To examine the antimicrobial activity of $Au_{25}(Capt)_{18}$ clusters on periodontal bacteria, we also meansured the turbidity of *A. actinomycetemcomitans* and *P. gingivalis*. These results are shown in Figs. 4E and 4F. Interestingly, addition of $Au_{25}(Capt)_{18}$ clusters consistently lowered the turbidity of bacterial suspensions, regardless of the application of blue LED irradiation, in contrast to assessment in *S. mutans*. The combination of $Au_{25}(Capt)_{18}$ clusters and LED irradiation significantly reduced the turbidity of *A.*

actinomycetemcomitans and P. gingivalis, especially for 50 and 500μg/ml $Au_{25}(Capt)_{18}$ clusters compared to the cases of other samples.

3.4. Cytotoxic effect of $Au_{25}(Capt)_{18}$ clusters and blue LED light

In order to examine the cytotoxicity of $Au_{25}(Capt)_{18}$ clusters and blue LED light irradiation, SEM observation, vinculin-F-actin staining and live/dead staining were performed for two cell lines: NIH3T3 and MC3T3-E1 cells. The morphology of incubated NIH3T3 and MC3T3-E1 cells was equivalent between examination and control groups in SEM images (Figs. 5A-D). Vinculin and F-actin were expressed as cell attachment and spreading with fine process elongation; pseudopod, were detected regardless of $Au_{25}(Capt)_{18}$ clusters and blue LED irradiation (Figs. 5E-H). In addition, live/dead assay showed that all samples consistently exhibited green fluorescence (Figs. 5I-L).

The results of WST-8 and LDH assays are presented in Fig. 6. At 2 days, cells were equivalently proliferated regardless of the application of $Au_{25}(Capt)_{18}$ clusters under blue LED irradiation. However, at 4 and 6 days of NIH3T3 cells and at 6 days of MC3T3-E1 cells, cell proliferation was significantly down-regualted by $Au_{25}(Capt)_{18}$ clusters application in a dose dependent manner. In particular, the combination of the $Au_{25}(Capt)_{18}$ clusters and blue LED irradiation suppressed cell viability stronger than that of

$Au_{25}(Capt)_{18}$ clusters only treatment. LDH assay showed that 50 and 500 μg/ml $Au_{25}(Capt)_{18}$ clusters enhanced LDH activity 2 days after incubation. In contrast, low dose, 5 μg/ml $Au_{25}(Capt)_{18}$ clusters, showed low LDH activity and no significant difference compared to control.

3.5 Comparative cytotoxic evaluations of $Au_{25}(Capt)_{18}$ clusters and MB

SEM and fluorescence microscope images of NIH3T3 and MC3T3E1 cells receiving photosensitizers (under non-LED irradiation condition) are shown in Figs. 7A-L. Following 10 and 100 μg/mL MB application, cell spreading, including the development of stress fibers and expression of vinculin, were significantly inhibited when compared to 500μg/mL $Au_{25}(Capt)_{18}$ clusters receiving group. In particular, the ball-shaped cells were observed by addition of 100 μg/mL MB (Figs. 7C, F, I, L). The result of WST-8 assay is shown in Figs. 8A and B. Application of $Au_{25}(Capt)_{18}$ clusters consistently stimulated the proliferation of the cells compared to the MB. Marked suppression of cell viability was observed on 100 μg/mL MB application.

The turbidity of *A. actinomycetemcomitans* and *P. gingivalis* was strongly decreased on application of 500μg/mL $Au_{25}(Capt)_{18}$ clusters or 10 and 100 μg/mL MB (Fig. 8C, D). After all, 100 μg/mL MB exhibited greatest antimicrobial effect among

those examined here, although MB has higher cytotoxicity than $Au_{25}(Capt)_{18}$ clusters. The turbidity of samples receiving 500μg/mL $Au_{25}(Capt)_{18}$ clusters exhibited no significant difference compared to 10 μg/mL MB.

4. Discussion

Blue LED are already widespread for the polymerization of composite resins. Further, Chui et al.[20] reported that blue LED greatly suppressed gene expression associated with DNA replication and bacterial cell division compared to red LED, resulting in inhibition of *P. gingivalis*. Therefore, the blue light source in aPDT might provide a favorable auxiliary for antimicrobial effect. In this study, blue LED irradiation alone slightly increased antimicrobial effect and LDH activity in this assessment. Since $Au_{25}(Capt)_{18}$ clusters possess strong absorbance in the wave length region of blue LED light, the antimicrobial effect of $Au_{25}(Capt)_{18}$ clusters may be promoted by the coupling effect of blue LED light-induced production of $^1O_2$ and the action of blue light.

Antimicrobial assessments revealed that turbidity and viability of *S. mutans* were gradually reduced by application of $Au_{25}(Capt)_{18}$ clusters under blue LED light in a cluster dose- and irradiation time-dependent manner. On SEM observation, bacterial colonies were fewer in the photoexcited $Au_{25}(Capt)_{18}$ clusters receiving group when

compared to control. It is likely that $^1O_2$ generated by photoexcited $Au_{25}(Capt)_{18}$ clusters suppressed *S. mutan*s growth and bacterial clump formation. Live/dead staining observation revealed that dead bacteria were significant in the samples applied with photoexcited Au clusters. In addition, we frequently found *S. mutans* with an irregular cell wall in TEM images (Fig. 3), which suggested that the bacteria cell wall was destroyed by the $^1O_2$, consequently cell death was stimulated. In general, as $^1O_2$ quickly disappears in about 3.5 μ sec following its generation[19], the distance of $^1O_2$ diffusion to the bacterial cells is a very important factor that affects aPDT activity. Fluorescent examination revealed that $Au_{25}(Capt)_{18}$ clusters in culture medium agglutinated around *S. mutans* (Fig. 3B). Accordingly, we assume that Au clusters attach to the bacterial cells and persistently provide $^1O_2$ to *S. mutans*, thus exerting an antimicrobial effect. The lactic acid production of *S. mutans* was also inhibited by photoexcited Au clusters, similar to bacterial growth. The reduction of lactic acid production may have been associated with inhibition of *S. mutans* growth. Conversely, previous reports revealed that the metabolic function of bacterial cell was downregulated by $^1O_2$ *via* oxidation of amino acid[25] or damage of DNA[26]. Therefore, application of $Au_{25}(Capt)_{18}$ clusters under blue LED light would be beneficial for PDT against *S. mutans*.

The combined application of $Au_{25}(Capt)_{18}$ clusters and light irradiation strongly diminished the turbidity of periodontal bacterial suspensions; *A. actinomycetemcomitans* and *P. gingivalis*, suggesting that photoexcited Au clusters consistently exhibited an antibacterial effect on the periodontal bacteria. According to the report of Bhatti et al.[27], $^1O_2$ showed sufficient effectiveness on gram-negative bacteria including *A. actinomycetemcomitans* and *P. gingivalis* as well as gram-positive bacteria; *S. mutans*. Even in low concentration of $Au_{25}(Capt)_{18}$ clusters (5 μg/ml), application of the Au clusters was effective against *A. actinomycetemcomitans* and *P. gingivalis*. In addition, the no irradiation group showed reduction of turbidity of periodontal bacterial suspensions. Since the culture medium including $Au_{25}(Capt)_{18}$ clusters was exposed to visible light in this study, a small amount of $^1O_2$ might be created which affected the bacterial growth. Antibacterial effect against not only gram negative but gram positive bacterial cells was exerted. From these evidence showed in this study, the producing $^1O_2$ by $Au_{25}(Capt)_{18}$ clusters under blue LED light plays a major role in antimicrobial effect on oral flora in periodontal therapy. Some reports [28-30] showed that aPDT using dye-photosensitizers resisted plaque formation, suggesting that $^1O_2$ would penetrate dental plaque and subsequently causes the destruction of dental plaque.

In order to confirm the biocompatibility of $Au_{25}(Capt)_{18}$ clusters, we carried out the cytotoxic test in two types of cell lines associated with periodontal tissue[31, 32]. SEM images and live/dead staining after 24 h of culture showed that fibroblastic and osteoblastic cells receiving photoexcited $Au_{25}(Capt)_{18}$ clusters normally spread on the culture dish and fluoresced as live cells. In addition, expression of f-actin and vinculin, associated with cell adhesion, was demonstrated similar to control. It was suggested that $Au_{25}(Capt)_{18}$ clusters has no cytotoxicity. Normally, strong antibacterial activity lead to strong cytotoxicity. Cyto-compatibility of $Au_{25}(Capt)_{18}$ clusters would be advantageous for biomedical application. However, the application of Au clusters dose-dependently decreased cell viability and increased LDH after 4 days incubation, in particular, under conditions receiving light irradiation. It is considered that application of Au clusters in the long term would gradually exert cytotoxicity by $^1O_2$. When we utilize the $Au_{25}(Capt)_{18}$ clusters for aPDT, a short period application would be desirable for weakening of cytotoxicity. From the fact that photoexcited $Au_{25}(Capt)_{18}$ clusters at a concentration of 5 μg/mL well-suppressed the growth of periodontal bacteria and rarely inhibited growth of fibroblastic and osteoblastic cells after 2 days incubation, we concluded that 5 μg/mL Au clusters would be safe for periodontal aPDT.

We addressed the biocompatible properties of 500μg/mL $Au_{25}(Capt)_{18}$ clusters compared to 10 and 100 μg/mL MB which are used in conventional aPDT procedures. The result showed that *A. actinomycetemcomitans* and *P. gingivalis* turbidity receiving 500 μg/mL $Au_{25}(Capt)_{18}$ clusters was equivalent to those receiving 10 μg/mL MB, regardless of light irradiation. However, the viability of fibroblastic and osteoblastic cells was remarkably suppressed by application of MB compared to Au clusters. Furthermore, immunostaining examination indicated that MB caused poor cell spreading and vinculin expression compared to $Au_{25}(Capt)_{18}$ cluster application, in particular, 100 μg/mL MB showed strong cellular dysfunction. Thus, MB and its complex might decrease the cell adhesion and proliferation when mobilized in aPDT. As the effect of light irradiation was not evaluated, the direct interaction of organic substances with the bacteria might play a major role in cytotoxic effects.

5. Conclusion

The antimicrobial and cytocompatible effects of $Au_{25}(Capt)_{18}$ clusters under blue LED light irradiation were examined *in vitro*. Fluorescence measurement revealed that $^1O_2$ was generated when $Au_{25}(Capt)_{18}$ clusters were irradiated with blue LED light. Application of photoexcited $Au_{25}(Capt)_{18}$ clusters significantly inhibited the growth of

oral bacterial cells, including *S. mutans*, *A. actinomycetemcomitans*, and *P. gingivalis*. Even if we singly used blue LED, slight antibacterial effect was detected. In addition, $Au_{25}(Capt)_{18}$ clusters under blue LED rarely exhibited cytotoxicity in fibroblastic NIH3T3 and osteoblastic MC3T3E1 cells in particular, at low dose application. In comparison with a typical organic dye photosensitizer; MB, $Au_{25}(Capt)_{18}$ clusters were biosafe. Therefore, $Au_{25}(Capt)_{18}$ clusters and blue LED are expected to be beneficial for aPDT related to dental therapy.

References

1) Konopka K, Goslinski T: Photodynamis therapy in dentistry. J Dent Res 86 : 694-707, 2007.

2) Hamblin MR, Hasan T: Photodynamic therapy: a new antimicrobial approach to infectious disease? Photochem Photobiol Sci 3 : 436-450, 2004.

3) Henderson BW, Dougherty TJ: How does photodynamic therapy work? Photochem Photobiol 55 : 145-157, 1992.

4) El-Hussein A, Harith M, Abrahamse H: Assessment of DNA damage after photodynamic therapy using a metallophthalocyanine photosensitizer. International Journal of Photoenergy 2012 : 1-10, 2012.

5) Plaetzer K, Krammer B, Berlanda J, Berr F, Kiesslich T: Photophysics and photochemistry of photodynamic therapy: Fundamental aspects. Lasers Med Sci 24 : 259-268, 2009.

6) Wilson M: Lethal photosensitization of oral bacteria and its potential application in the photodynamic therapy of oral infections. Photochem Photobiol Sci 3 : 412-418, 2004.

7) Meisel P, Kocher T: Photodynamic therapy for periodontal diseases: State of the art. J Photochem Photobiol B 79 : 159-170, 2005.

8) Biel MA: Photodynamic therapy of bacterial and fungal biofilm infections. Methods Mol Biol 635 : 175-194, 2010.

9) Zanin IC, Gonçalves RB, Junior AB, Hope CK, Pratten J: Susceptibility of Streptococcus mutans biofilms to photodynamic therapy: an in vitro study. J Antimicrob Chemother 56 : 324-330, 2005.

10) Wood S, Metcalf D, Devine D, Robinson C: Erythrosine is a potential photosensitizer for the photodynamic therapy of oral plaque biofilms. J Antimicrob Chemother 57 : 680-684, 2006.

11) Rajesh S, Koshi E, Philip K, Mohan A: Antimicrobial photodynamic therapy: An overview. J Indian Soc Periodontol 15 : 323-327, 2011.

12) Prasanth CS, Karunakaran SC, Paul AK, Kussovski V, Mantareva V, Ramaiah D, Selvaraj L, Angelov I, Avramov L, Nandakumar K, Subhash N: Antimicrobial photodynamic efficiency of novel cationic porphyrins towards periodontal Gram-positive and Gram-negative pathogenic bacteria. Photochem Photobiol 90 : 628-640, 2014.

13) Soria-Lozano P, Gilaberte Y, Paz-Cristobal MP, Pérez-Artiaga L, Lampaya-Pérez V, Aporta J, Pérez-Laguna V, García-Luque I, Revillo MJ, Rezusta A: In vitro effect

photodynamic therapy with differents photosensitizers on cariogenic microorganisms. BMC Microbiol 15 : 187, 2015.

14) Parker S: The use of diffuse laser photonic energy and indocyanine green photosensitiser as an adjunct to periodontal therapy. Br Dent J 215 : 167-171, 2013.

15) Rosa LP, da Silva FC, Nader SA, Meira GA, Viana MS: Antimicrobial photodynamic inactivation of Staphylococcus aureus biofilms in bone specimens using methylene blue, toluidine blue ortho and malachite green: An in vitro study. Arch Oral Biol 60 : 675-680, 2015.

16) Christodoulides N, Nikodakis D, Chondros P, Becker J, Scwarz F, Rössler R,, Sculean A: Photodynamic therapy as an adjunct to non-surgical periodontal treatment: a randomized, controlled clinical trial. J Periodontal 79 : 1638-1644, 2008.

17) Moan J, Berg K: The photodegradation of porphyrins in cells that can be used to estimate the lifetime of singlet oxygen. Photochem Photobiol 53 : 549-553, 1991.

18) Crooks J: Haemolytic jaundice in a neonate after intra-amniotic injection of methylene blue. Arch Dis Child 57 : 872-873, 1982.

19) Kawasaki H, Kumar S, Li G, Zeng C, Kauffman DR, Yoshimoto J, Iwasaki Y, Jin R: Generation of singlet oxygen by photoexcited $Au_{25}(SR)_{18}$ Clusters. Chemistry of Materials 26 : 2777-2778, 2014.

20) Chui C, Hiratsuka K, Aoki A, Takeuchi Y, Abiko Y, Izumi Y: Blue LED inhibits the growth of Porphyromonas gingivalis by suppressing the expression of genes associated with DNA replication and cell division. Lasers Surg Med 44 : 856-864, 2012.

21) Kumar S, Jin R: Water-soluble $Au_{25}(Capt)_{18}$ nanoclusters: synthesis, thermal stability, and optical properties. Nanoscale 4 : 4222-4227, 2012.

22) Hirakawa K: Fluorometry of singlet oxygen generated via a photosensitized reaction using folic acid and methotrexate. Anal.Bioanal.Chem 393 : 999-1005, 2009.

23) Javed F, Romanos GE: Does photodynamic therapy enhance standard antibacterial therapy in dentistry? Photomed Laser Surg 31 : 512-518, 2013.

24) Almeida JM, Theodoro LH, Bosco AF, Nagata MJ, Oshiiwa M, Garcia VG: In vivo effect of photodynamic therapy on periodontal bone loss in dental furcations. J Periodontal 79 : 1081-1088, 2008.

25) Agnez-Lima LF, Melo JT, Silva AE, Oliveira AH, Timoteo AR, Lima-Bessa KM, Martinez GR, Medeiros MH, Di Mascio P, Galhardo RS, Menck CF: DNA damage by singlet oxygen and cellular protective mechanisms. Mutatat Res 751 : 15-28, 2012.

26) Bhatti M, MacRobert A, Meghji S, Henderson B, Wilson M: A study of the uptake of toluidine blue O by Porphyromonas gingivalis and the mechanism of lethal photosensitization. Phoyochem Photobiol 68 : 370-376, 1998.

27) Pivodova V, Frankova J, Ulrichova J: Osteoblast and gingival fibroblast markers in dental implant studies. Biomed Pap Med Fac Univ Palacky Olomouc Czech Repub 155 : 109-116, 2011.

28) Ichinose-Tsuno A, Aoki A, Takeuchi Y, Kirikae T, Shimbo T, Lee MC, Yoshino F, Maruoka Y, Itoh T, Ishikawa I, Izumi Y: Antimicrobial photodynamic therapy suppresses dental plaque formation in healthy adults: a randomized controlled clinical trial. BMC Oral Health 14 : 152, 2014.

29) Fontana CR, Abernethy AD, Som S, Ruggiero K, Doucette S, Marcantonio RC, Boussios CI, Kent R, Goodson JM, Tanner AC, Soukos NS: The antibacterial effect of photodynamic therapy in dental plaque-derived biofilms. J Periodontal Res 44 : 751-759, 2009.

30) O'Neill JF, Hope CK, Wilson M: Oral bacteria in multispecies biofilms can be killed by red light in the presence of toluidine blue. Lasers Surg Med 31 : 86-90, 2002.

31) Lekic P, McCulloch CA: Periodontal ligament cell populations: The central role of fibroblasts in creating a unique tissue. Anat Rec 245 : 327-341, 1996.

Maisch T, Baier J, Franz B, Maier M, Landthaler M, Szeimies RM, Baumler W: The role of singlet oxygen and oxygen concentration in photodynamic inactivation of bacteria. Proc Natl Acad Sci USA 104 : 7223-7228, 2007.

Acknowledgments

This work was supported by JSPS KAKENHI (Grant No. JP15H03520, JP15H03526, JP26505011, JP26107719 and JP16K11822) and Hitachi Metals Materials Science Foundation. A part of this work was supported by the Nanotechnology Platform Program (Molecule and Material Synthesis) of the Ministry of Education, Culture, Sports, Science and Technology (MEXT), Japan.

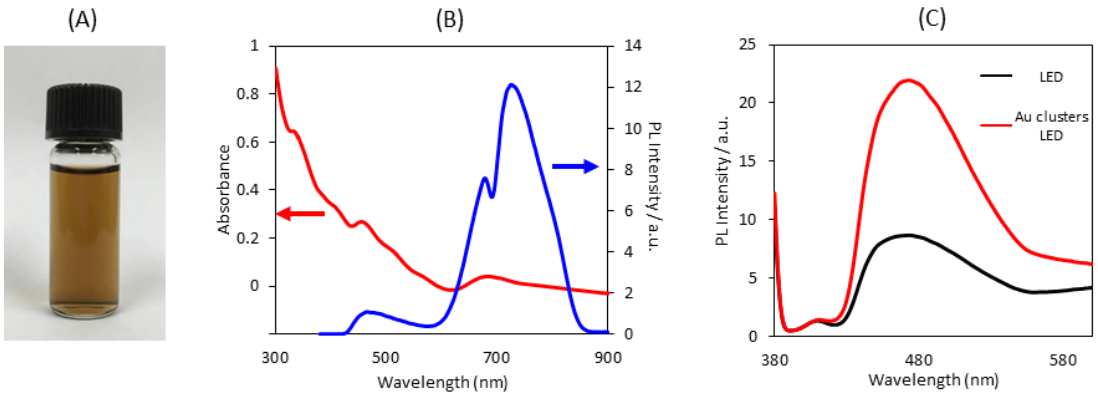
(A)
(B)
(C)
Absorbance
PL Intensity / a.u.
Wavelength (nm)
LED
Au clusters
LED
PL Intensity / a.u.
Wavelength (nm)

Fig. 1

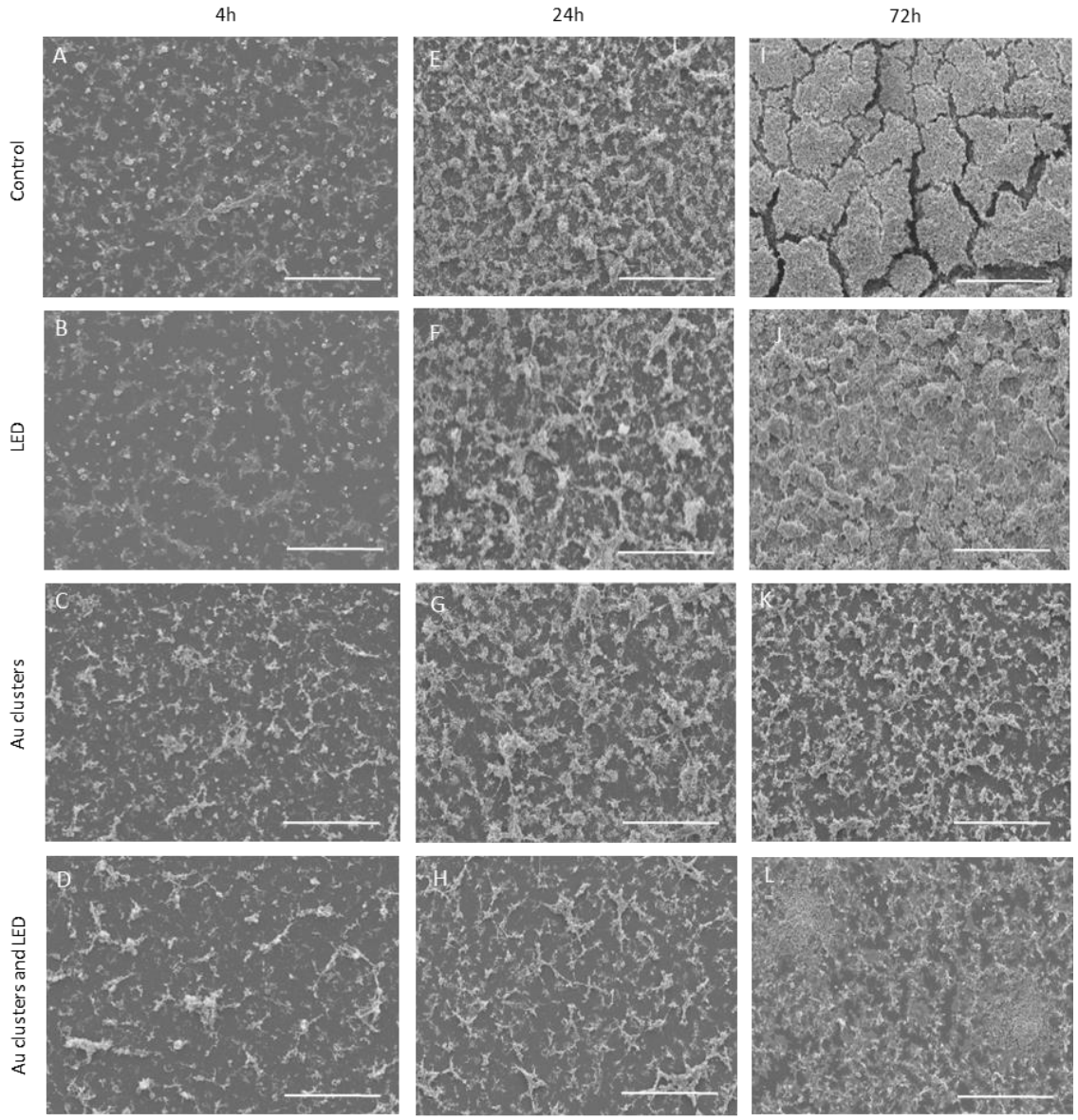
4h
24h
72h
Control
LED
Au clusters
Au clusters and LED
A
E
I
B
F
J
C
G
K
D
H
L

Fig. 2

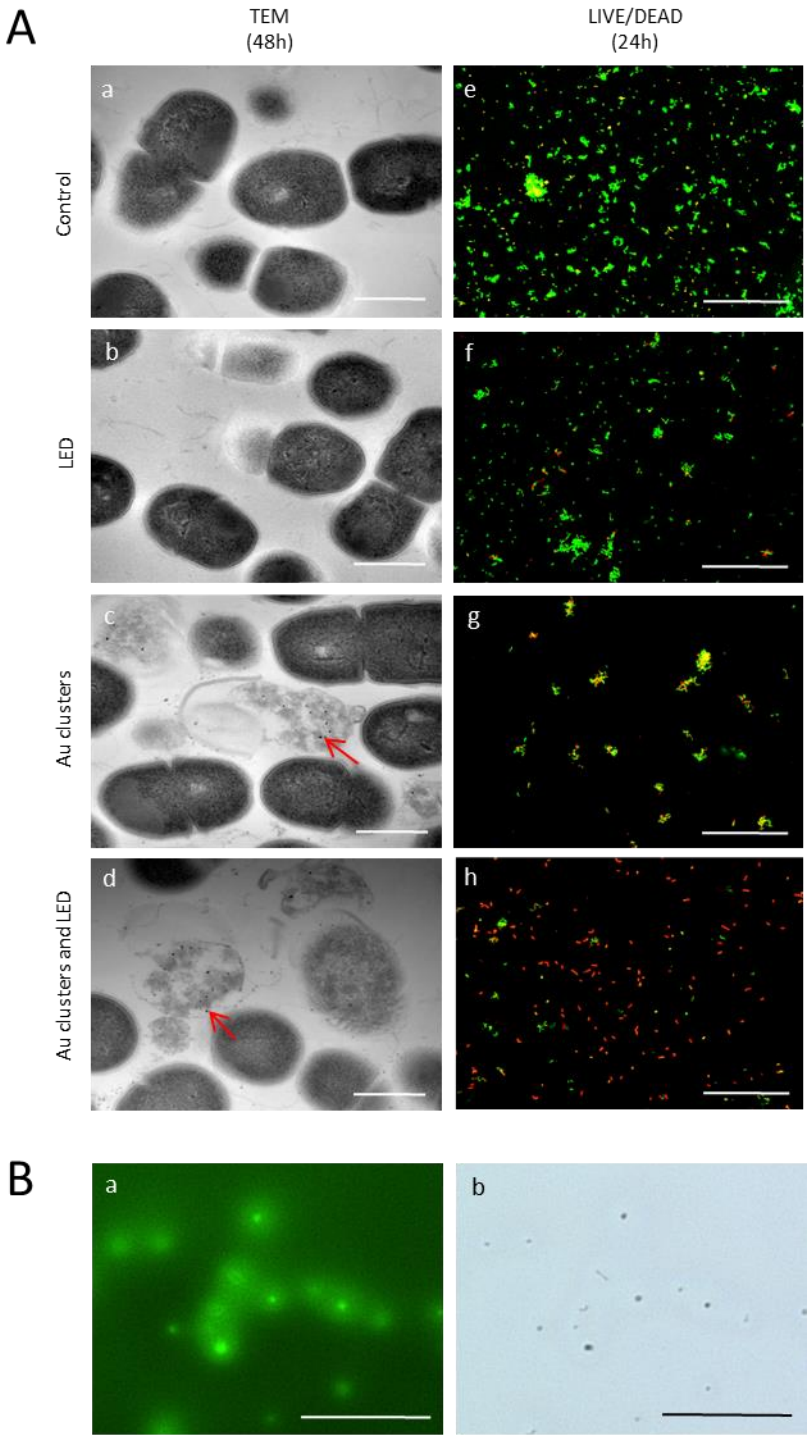
A
TEM
(48h)
LIVE/DEAD
(24h)
Control
LED
Au clusters
Au clusters and LED
a
b
c
d
e
f
g
h
B
a
b

Fig. 3

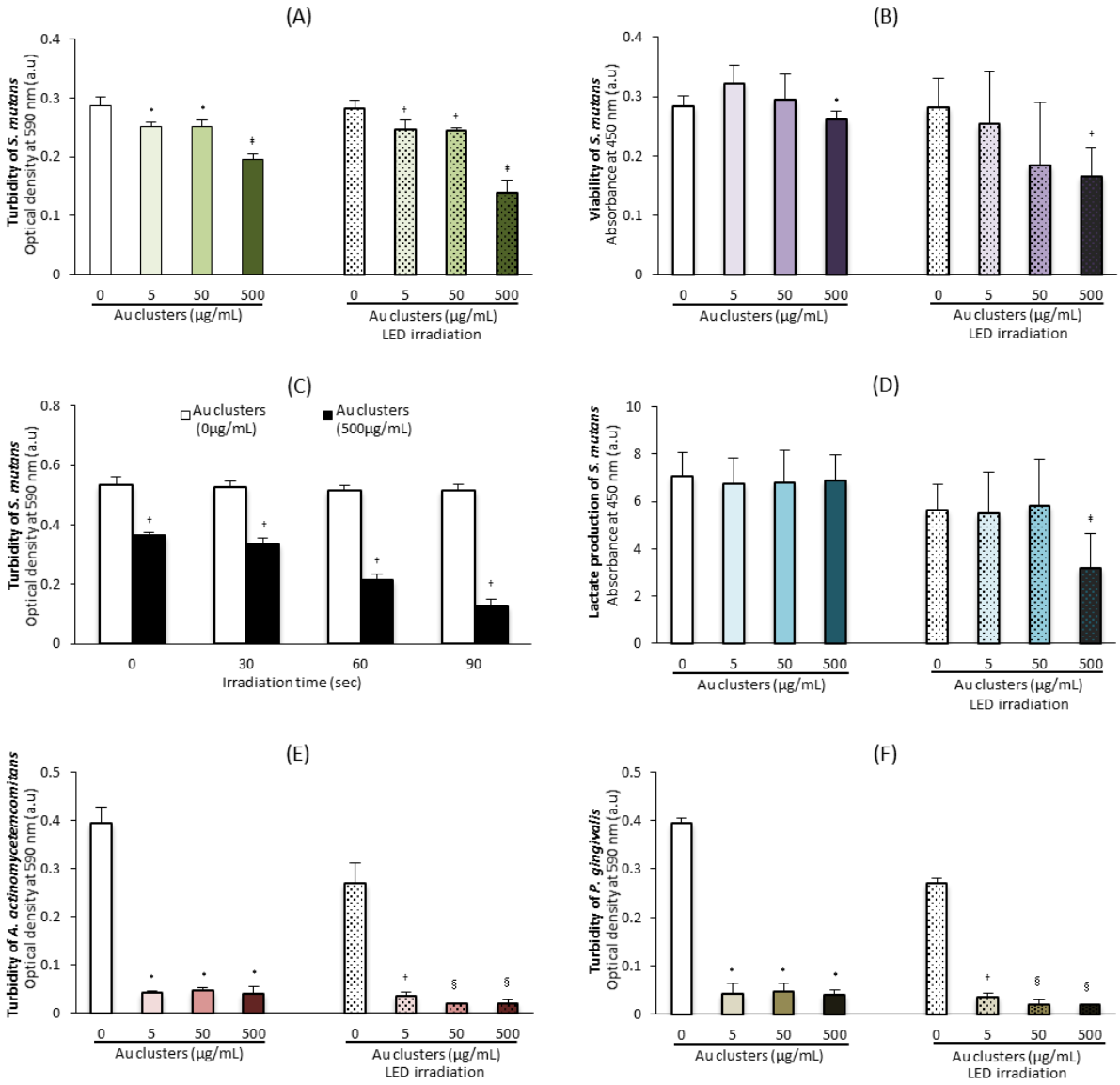
(A)
Turbidity of S. mutans
Optical density at 590 nm (a.u)
0.4
0.3
0.2
0.1
0
0 5 50 500
Au clusters (μg/mL)
0 5 50 500
Au clusters (μg/mL)
LED irradiation
(B)
Viability of S. mutans
Absorbance at 450 nm (a.u)
0.4
0.3
0.2
0.1
0
0 5 50 500
Au clusters (μg/mL)
0 5 50 500
Au clusters (μg/mL)
LED irradiation
(C)
Au clusters (0μg/mL)
Au clusters (500μg/mL)
Turbidity of S. mutans
Optical density at 590 nm (a.u)
0.8
0.6
0.4
0.2
0
0 30 60 90
Irradiation time (sec)
(D)
Lactate production of S. mutans
Absorbance at 450 nm (a.u)
10
8
6
4
2
0
0 5 50 500
Au clusters (μg/mL)
0 5 50 500
Au clusters (μg/mL)
LED irradiation
(E)
Turbidity of A. actinomycetemcomitans
Optical density at 590 nm (a.u)
0.5
0.4
0.3
0.2
0.1
0
0 5 50 500
Au clusters (μg/mL)
0 5 50 500
Au clusters (μg/mL)
LED irradiation
(F)
Turbidity of P. gingivalis
Optical density at 590 nm (a.u)
0.5
0.4
0.3
0.2
0.1
0
0 5 50 500
Au clusters (μg/mL)
0 5 50 500
Au clusters (μg/mL)
LED irradiation

Fig. 4

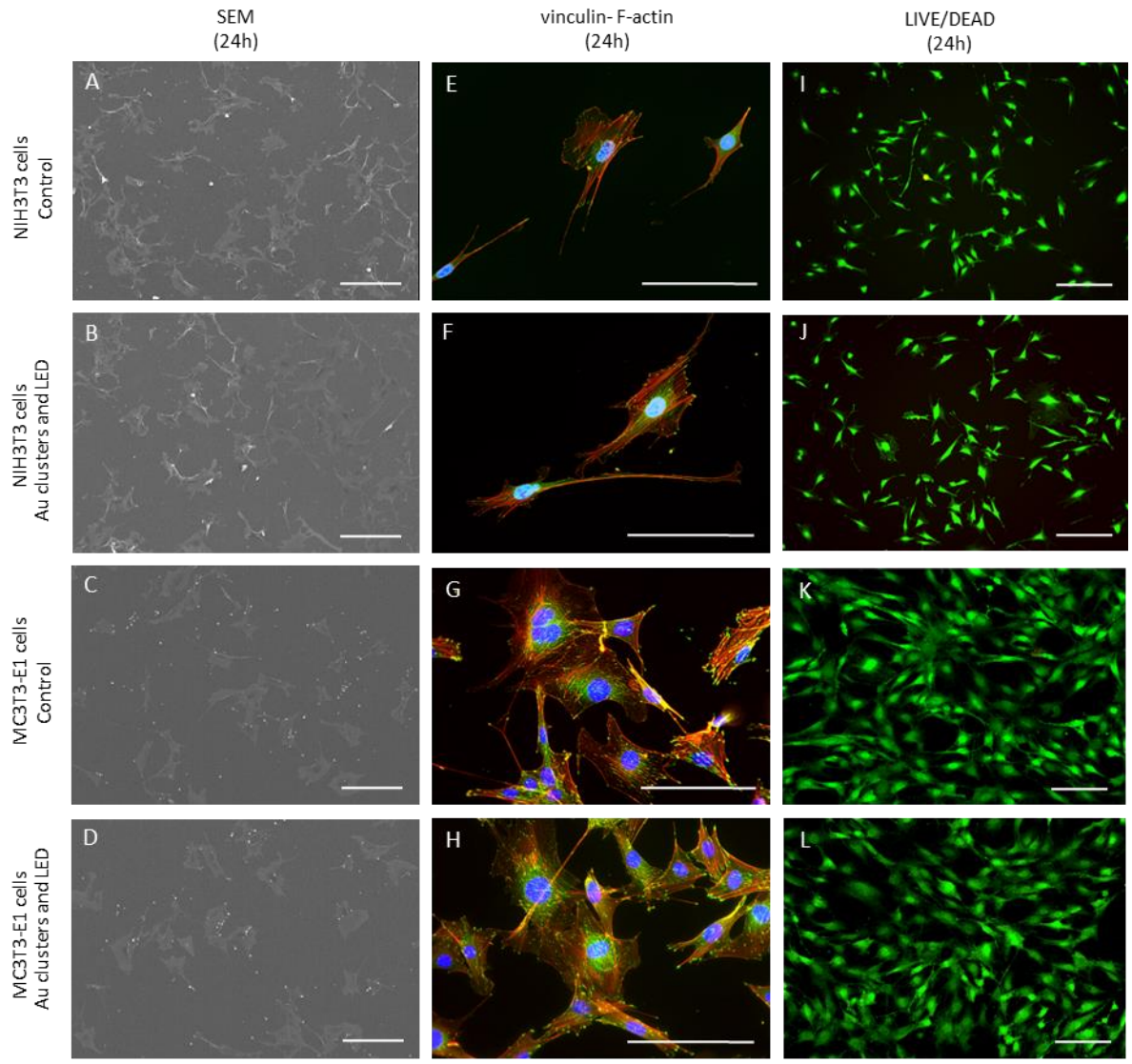
SEM
(24h)
vinculin- F-actin
(24h)
LIVE/DEAD
(24h)
NIH3T3 cells
Control
NIH3T3 cells
Au clusters and LED
MC3T3-E1 cells
Control
MC3T3-E1 cells
Au clusters and LED
A
B
C
D
E
F
G
H
I
J
K
L

Fig. 5

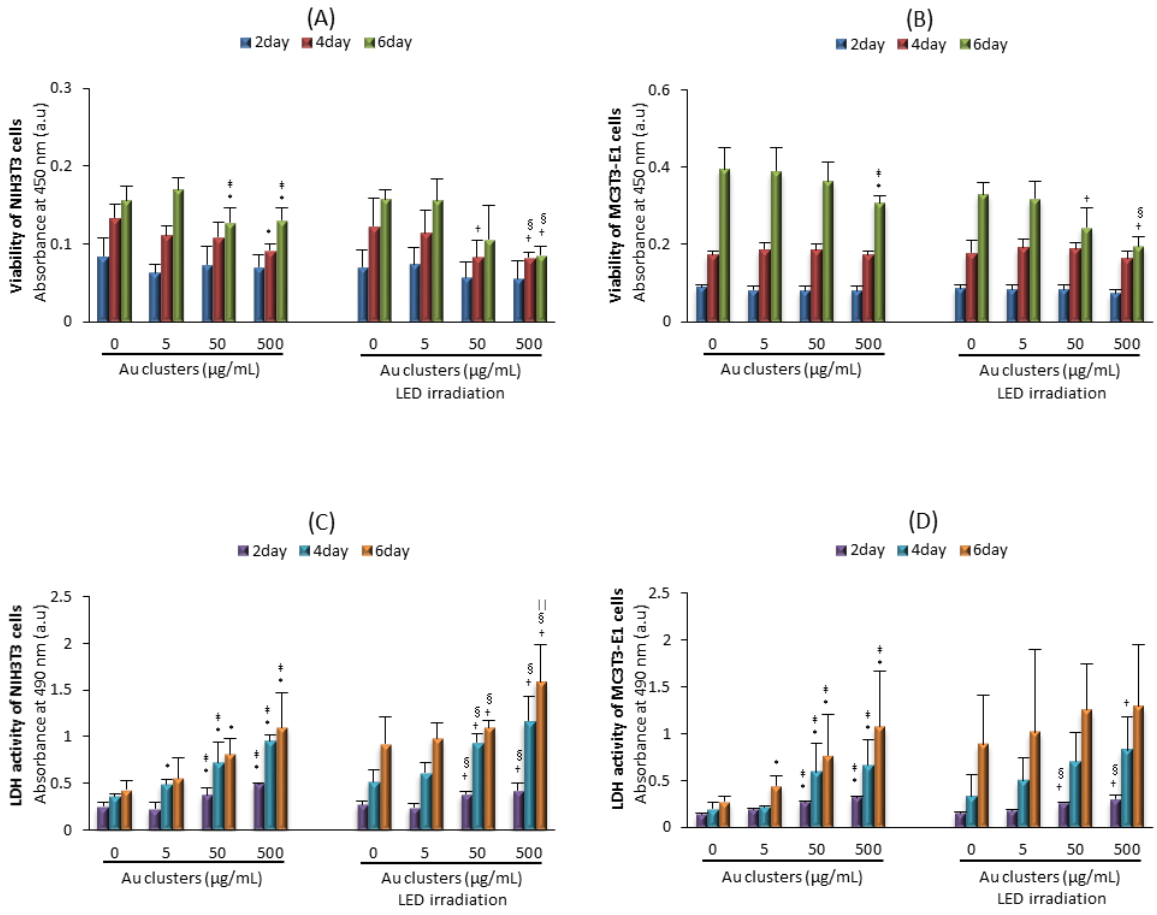
(A)
2day 4day 6day
Viability of NIH3T3 cells
Absorbance at 450 nm (a.u)
0.3
0.2
0.1
0
0 5 50 500
Au clusters (μg/mL)
0 5 50 500
Au clusters (μg/mL)
LED irradiation
(B)
2day 4day 6day
Viability of MC3T3-E1 cells
Absorbance at 450 nm (a.u)
0.6
0.4
0.2
0
0 5 50 500
Au clusters (μg/mL)
0 5 50 500
Au clusters (μg/mL)
LED irradiation
(C)
2day 4day 6day
LDH activity of NIH3T3 cells
Absorbance at 490 nm (a.u)
2.5
2
1.5
1
0.5
0
0 5 50 500
Au clusters (μg/mL)
0 5 50 500
Au clusters (μg/mL)
LED irradiation
(D)
2day 4day 6day
LDH activity of MC3T3-E1 cells
Absorbance at 490 nm (a.u)
2.5
2
1.5
1
0.5
0
0 5 50 500
Au clusters (μg/mL)
0 5 50 500
Au clusters (μg/mL)
LED irradiation

Fig. 6

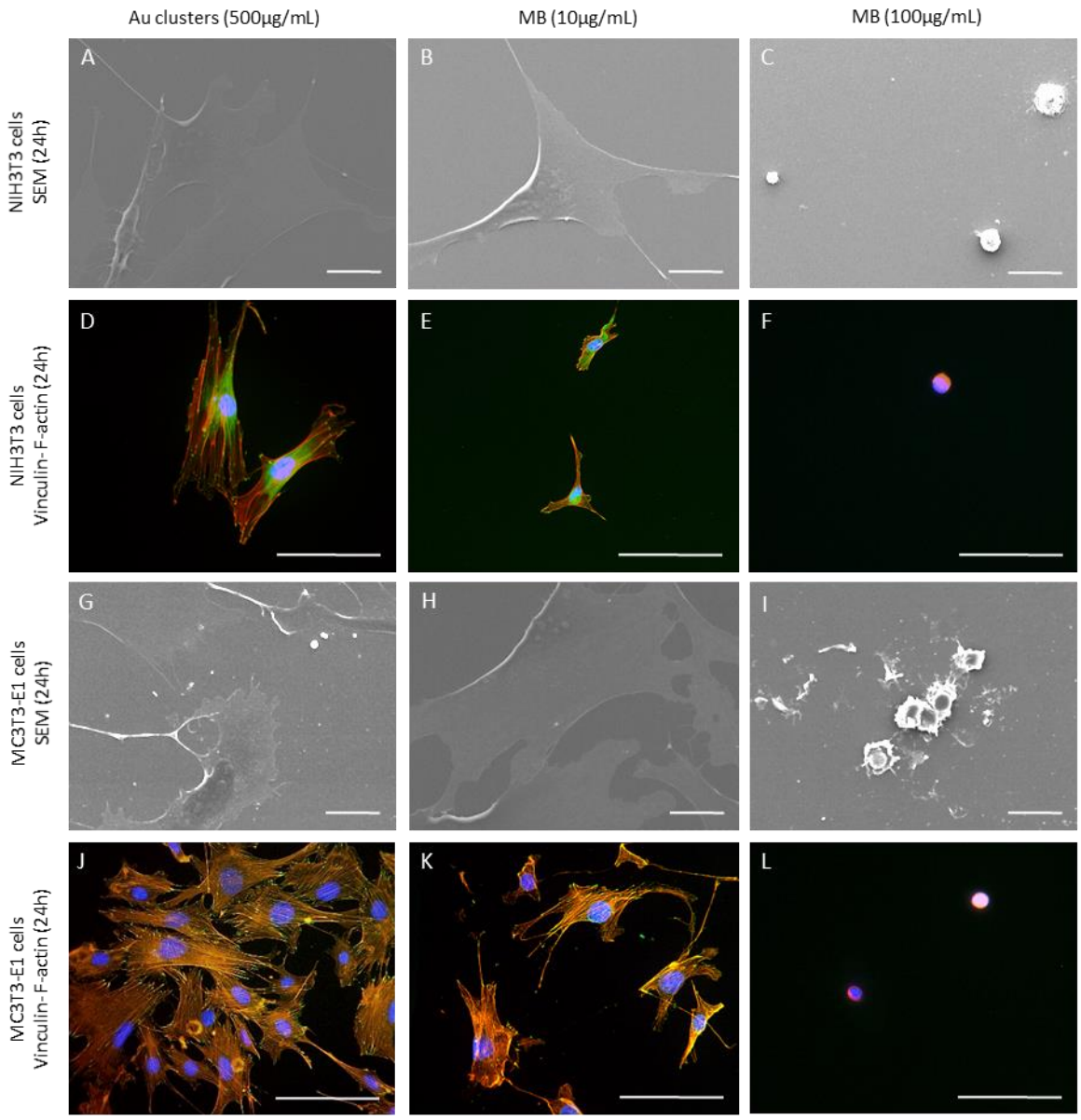
Au clusters (500µg/mL)
MB (10µg/mL)
MB (100µg/mL)
NIH3T3 cells SEM (24h)
NIH3T3 cells Vinculin-F-actin (24h)
MC3T3-E1 cells SEM (24h)
MC3T3-E1 cells Vinculin-F-actin (24h)
A
B
C
D
E
F
G
H
I
J
K
L

Fig. 7

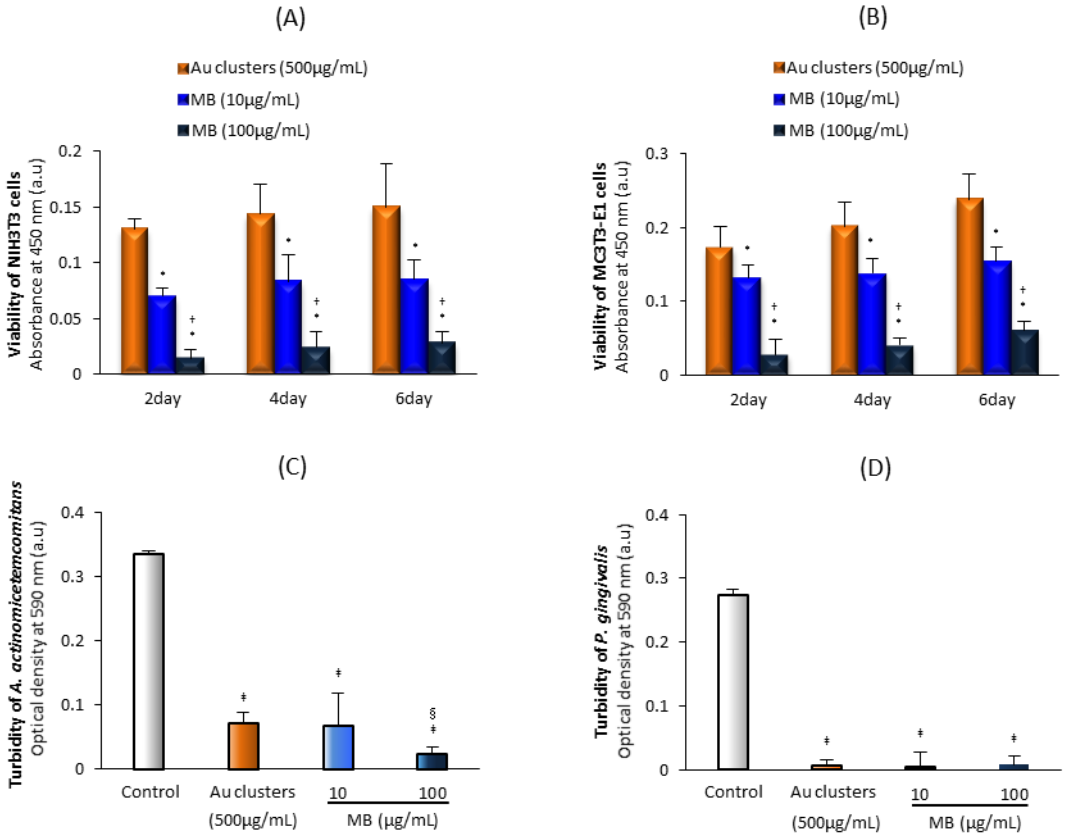
(A)
Au clusters (500μg/mL)
MB (10μg/mL)
MB (100μg/mL)
Viability of NIH3T3 cells
Absorbance at 450 nm (a.u)
0.2
0.15
0.1
0.05
0
2day
4day
6day
(B)
Au clusters (500μg/mL)
MB (10μg/mL)
MB (100μg/mL)
Viability of MC3T3-E1 cells
Absorbance at 450 nm (a.u)
0.3
0.2
0.1
0
2day
4day
6day
(C)
Turbidity of A. actinomicetemcomitans
Optical density at 590 nm (a.u)
0.4
0.3
0.2
0.1
0
Control
Au clusters (500μg/mL)
10
100
MB (μg/mL)
(D)
Turbidity of P. gingivalis
Optical density at 590 nm (a.u)
0.4
0.3
0.2
0.1
0
Control
Au clusters (500μg/mL)
10
100
MB (μg/mL)

Fig. 8

Figure legends

Fig. 1. Optical properties of $Au_{25}(Capt)_{18}$ clusters

(A) Aqueous solution of dispersed $Au_{25}(Capt)_{18}$ clusters. (B) The UV-Vis wavelength spectrum (red line) and Fluorescence spectrum (blue line) of $Au_{25}(Capt)_{18}$ clusters. (C) Fluorescence spectra of a MTX-containing solution of $Au_{25}(Capt)_{18}$ clusters.

Fig. 2: SEM observation of *S. mutans*

(A-L) SEM micrographs of *S. mutans* after 4 h (A-D), 24 h (E-H) and 72 h (I-L) incubation. Scale bar represents 100 μm (A-L). Au clusters application and LED irradiation diminished bacterial accumulation and biofilm formation compared to control (no application of Au clusters and no light irradiation) and LED light alone.

Fig. 3. Morphological and fluorescent examinations of *S. mutans*

(A) TEM micrographs (48 h incubation, a-d) and live/dead assay (24 h incubation, e-h) of *S. mutans*. Arrows (c, d) indicate ultrafine particles. (B) Fluorescent examination of labeled Au clusters. Fluorescent image (a) and light field image (b). Scale bar represents 1 μm (A (a-d)), 50 μm (A (e-h and B).

Fig. 4. Antimicrobial effects on oral bacterial cells after 24 h incubation (n=6, mean ± SD)

(A) Turbidity of *S. mutans*. (B) Viability of *S. mutans*. (C) Turbidity of *S. mutans* related to irradiation time. (D) Lactate production of *S. mutans*. (E) Turbidity of *A. actinomycetemcomitans*. (F) Turbidity of *P. gingivalis*: *, $P<0.05$ vs. 0 μg/mL Au clusters, †, $P<0.05$ vs. 0 μg/mL Au clusters after LED irradiation, ‡, $P<0.05$ vs. all other subjects and §, $P<0.05$ vs. 0 and 5 μg/mL Au clusters after LED irradiation.

Fig. 5. Evaluation of cell morphology after 24 h incubation.

(A-D) SEM observation. (E-H) vinculin- F-actin fluorescent double staining. (I-L) Live/dead staining. Scale bar represents 200 μm (A-D), 50 μm (E-H), and 100 μm (I-L). The morphology of NIH3T3 and MC3T3-E1 cells following Au clusters application and LED irradiation was similar to control (no application of Au clusters and no light irradiation).

Fig. 6. Cytotoxic effects on fibroblastic and osteoblastic cells at 2, 4 and 6 days (n=6, mean ± SD).

(A) Viability of NIH3T3 cells. (B) Viability of MC3T3-E1 cells. (C) LDH activity of NIH3T3 cells. (D) LDH activity of MC3T3-E1 cells: *, $P<0.05$ vs. 0 μg/mL Au clusters, †, $P<0.05$ vs. 0 μg/mL Au clusters after LED irradiation, ‡, $P<0.05$ vs. 5 μg/mL Au clusters, §, $P<0.05$ vs. 5 μg/mL Au clusters after LED irradiation, ||, $P<0.05$ vs. 50 μg/mL Au clusters after LED irradiation.

Fig. 7. Comparative evaluation of cytotoxicity of $Au_{25}(Capt)_{18}$ clusters and MB after 24 h incubation

(A-C) SEM micrograph of NIH 3T3 cells. (D-F) vinculin-F-actin staining of NIH 3T3 cells. (G-I) SEM micrograph of MC3T3-E1 cells. (J-L) vinculin- F-actin staining of MC3T3-E1 cells. Scale bar represents 20 μm (A-C, G-I) and 50 μm (D-F, J-L).

Fig. 8. Cytotoxic and antimicrobial effects of $Au_{25}(Capt)_{18}$ clusters and MB

(A, B) Viability of NIH3T3 cells (A) and MC3T3-E1 cells (B) at 2, 4 and 6 days (n=5, mean ± SD): *, $P<0.05$ vs. 500 μg/mL Au clusters, †, $P<0.05$ vs. 10 μg/mL MB. (C, D) Turbidity assays of *A. actinomycetemcomitans* (C) and *P. gingivalis* (D) after 24 h incubation (n=5 mean ± SD): ‡, $P<0.05$ vs. control, §, $P<0.05$ vs. 500 μg/mL Au clusters and 10 μg/mL MB.